

# Search for neutral Supersymmetric Higgs bosons in di- $\tau$ and $b\tau\tau$ final states in $p\bar{p}$ collisions at $\sqrt{s} = 1.96$ TeV

Subhendu Chakrabarti

for D0 and CDF collaborations

Department of Physics and Astronomy, State University of New York, Stony Brook, NY, USA

We present a search for Higgs boson produced in the di-tau modes or via the associated  $p\bar{p} \rightarrow h + b \rightarrow \tau^+\tau^-b$  process at a center-of-mass energy of  $\sqrt{s} = 1.96$  TeV using up to  $1.8\text{-}7.3 \text{ fb}^{-1}$  of data collected with the D0 and CDF detector at the Fermilab Tevatron collider. In Supersymmetric models Higgs boson production cross section can be significantly enhanced compared to the Standard Model. Additionally the Higgs boson has a significant branching ratio to  $\tau$  leptons at all masses. The di- $\tau$  and  $b - \tau\tau$  channels complement each other providing best sensitivity for the search in the SUSY parameter space.

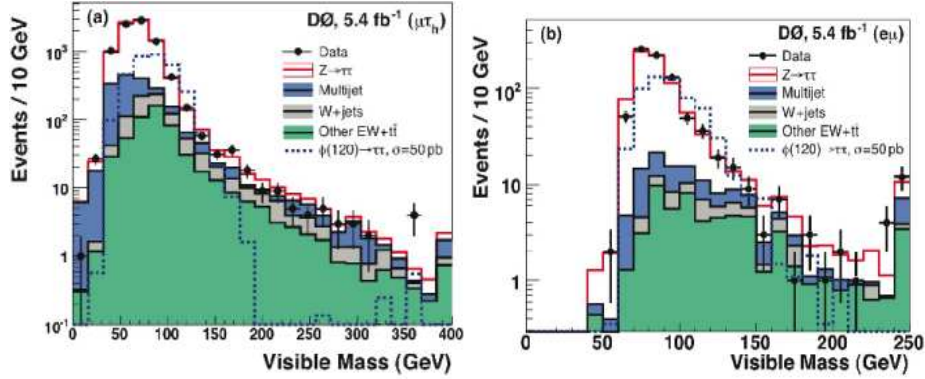
## I. INTRODUCTION

In the minimal supersymmetric standard model (MSSM), two complex Higgs bosons doublets can exist unlike only one standard model Higgs [1]. These doublets lead to five physical Higgs bosons: two neutral CP-even (h,H), one neutral CP-odd (A) and two charged Higgs Bosons ( $H^\pm$ ). The three neutral Higgs bosons are collectively called as  $\phi$ . At the tree level, Higgs sector of the MSSM are controlled by two parameters, which are the mass of the CP-odd Higgs bosons  $M_A$ , and the ratio of the vacuum expectation values of the two Higgs doublets,  $\tan \beta$ . The neutral bosons decay into  $\tau^+\tau^-$  and  $b\bar{b}$  pairs with branching fractions 10% and 90%. The neutral bosons also can decay in association with b quarks which lead to complimentary search channels to inclusive production. The production cross-section is enhanced by a factor that depends on  $\tan \beta$  than the standard model Higgs boson cross-section of the same mass. Also, for large  $\tan \beta$ , the Higgs Boson A and either h or H are nearly degenerate in mass which leads to an approximate doubling of production cross-section. In this paper, we present summary of MSSM neutral Higgs bosons searches with the data collected by D0 and CDF detector, described in [2] at the Tevatron involving  $\tau$  leptons. These searches are complimentary to searches with  $b\bar{b}$  pairs which is leading decay mode. Despite lower branching ratio, searches with  $\tau^+\tau^-$  pair have other advantages that they are not suppressed with huge multijet and large di-jet background. Moreover, neutral Higgs production in association with b quarks has the advantage to use the information of tagged b quarks to suppress irreducible  $Z$ +jets background.

## II. INCLUSIVE HIGGS BOSON SEARCHES

In this section, we briefly describe the search for neutral Higgs bosons which requires reconstruction of muons or electrons and atleast one hadronic decays of  $\tau$  lepton ( $\tau_{had}$ ) and missing transverse energy. A details description can be found elsewhere [3]. The data considered in this analysis were recorded by the D0 detector and correspond to an integrated luminosity of  $5.4 \text{ fb}^{-1}$  for the channel. Electron are reconstructed using their characteristic energy deposits and the shower shape in the calorimeter. Muons are identified from track segments in the muon system that are spatially matched to reconstructed in the muon system. Hadronic  $\tau$  decays are reconstructed from energy deposits in the calorimeter using a jet cone algorithm. The  $\tau$  candidates are then split into three categories which roughly correspond to one-prong  $\tau$  decay with no  $\pi^0$  (type 1), one-prong decay with  $\pi^0$  (type 2) and multiprong decay (type 3). In additional, we use a neural-network based  $\tau$  identification to separate jets from real  $\tau$  production. The  $NN_\tau$  is based on shower shape variables, isolation variables and correlation variables between tracking and calorimeter energy measurements.

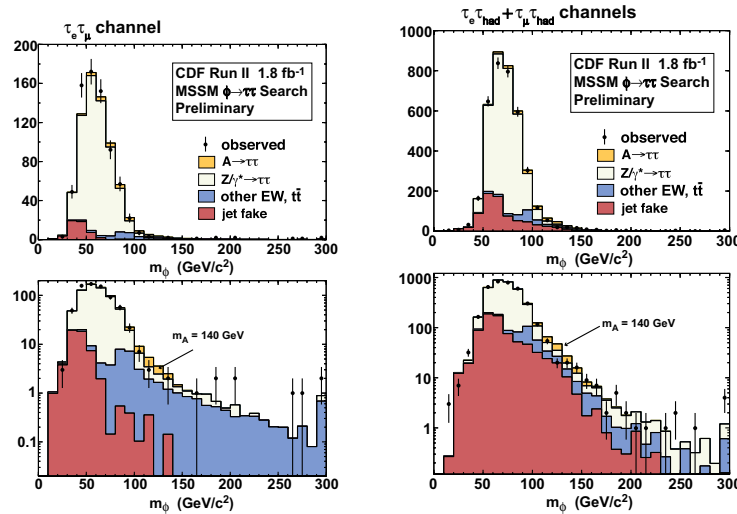
Events are selected by requiring at least one single muon trigger for the  $\mu\tau_h$  channel, while for the  $e\mu$  channel, they need to fulfill either inclusive electron and muon trigger conditions. The preselection sample is dominated by  $Z$ +jets,  $W$ +jets and MJ backgrounds. To reject  $Z\gamma \rightarrow \mu\mu$  and  $W$ +jets background events, further selection cuts  $\delta(\tau, \mu) > 0.5$  and transeverse mass of muon and missing energy  $> 50$  are applied. In the  $e\mu$  channel, events with atleast one muon with an oppositely electron are selected. Multijet background and W boson production is suppressed by requiring the mass of  $e\mu$  pair to be larger than 20 GeV and sum of missing transverse energy and transverse momentum of electron and muon  $> 65$  GeV. Requiring the scalar sum of the transverse momenta of all jets to be  $< 70$  GeV rejects a large fraction of  $t\bar{t}$  events. Shape of multijet background is estimated from same-sign data reversing the NN cut on  $\tau s$ . For  $e\mu$  channel, electron likelihood and muon isolation

FIG. 1: Visible mass distribution is shown.  $\mu\tau_h$  on left and  $e\mu$  on right

criteria is inverted to obtain the multijet background shape. After event selection, the number of expected SM background events (the number of observed data) are 8782 (8774), 830 (825) for the  $\mu\tau_h$  channel and  $e\mu$  channel. The signal efficiency from these channels is 1.16% (0.2%). After imposing all selection requirements, a variable called visible mass is reconstructed which is calculated using the four-vectors of the measured tau-lepton decay products. Distributions for the visible mass variable are shown in Fig. 1.

Several sources of systematics uncertainty affect the signal efficiency and background estimation. Largest systematics sources are integrated luminosity (6.1%), muon identification (2.9%), tau identification (12%, 4.2%, 7% per  $\tau$ -type), electron identification (2.5%),  $Z$ +jets cross-sections (5%),  $W$ +jets cross-sections (10-20%) and modeling of multijet background (9.1%, 17.7%, 12.5 per  $\tau$ -type).

CDF detector also performed this search for inclusive production of neutral Higgs bosons using data correspond to an integrated luminosity of  $1.8 \text{ fb}^{-1}$  [4]. CDF considered  $\text{di}\tau$  pairs in three final states which require reconstruction of electron, muons and hadronic decays of  $\tau$  lepton ( $\tau_{had}$ ).

FIG. 2: Visible mass distribution is shown.  $\mu\tau_h$ ,  $e\tau_h$  on right and  $e\mu$  on left

The events for the electron or muons and atleast one hadronic decays of  $\tau$  required to have lepton plus track triggers. They also require a lepton candidate and an isolated track with tranverse momentum  $p_T > 5 \text{ GeV}$ , both pointing the central detector ( $|\eta| \geq 1$ ) and having azimuthal separation  $\delta\phi > 10^\circ$ . In the CDF, the decay products in  $\tau_{had}$  appear as narrow jets with low track and  $\pi^0$  multiplicity. Reconstruction of  $\tau_{had}$  use a seed track and contiguous towers in the EM calorimeter for a tau candidate. The dominant background is  $Z$ +jets which can come from a  $Z\gamma$  production with subsequent decay to  $\tau$  pair. The second-largest contribution is from backgrounds from multijet or di-jet events where jets arising form quark or gluon fake as taus. There are also another set of standard model backgrounds which include  $Z$ ,  $WW$ ,  $WZ$ ,  $ZZ$ ,  $W\gamma$ ,  $Z\gamma$  and  $t\bar{t}$  production. The number of expected SM background events (the number of observed data) are 1921.1 (1979), 1750.8 (1666) and

701.9 (726). The combined signal detection efficiency from three channels for a Higgs boson of mass 90 GeV (250) is 1.0% (3.1%). To probe for possible Higgs mass, we performed binned likelihood fits for the partial reconstructed mass of di- $\tau$  ( $m_{vis}$ ) as shown in Fig. 2.

Several sources of systematic uncertainty also considered in this analysis. Major contribution comes from multijet background estimation (20%,15%), for  $\mu(e)\tau_h$  and  $e\mu$  channels. Also PDF's introduce 5.7% systematics and integrated luminosity contributes (6.1%) systematics +with minor contributions from electron and  $\tau$  identifications.

### III. HIGGS BOSON SEARCHES IN ASSOCIATION OF A B QUARK

In this section, we briefly describe the search for neutral Higgs bosons production in association with a b quark. The channel can produce electron or muons from leptonic  $\tau$  decay, hadronic decays of  $\tau$  lepton ( $\tau_{had}$ ) and a b quark jet [5]. The data considered in these analyses were recorded by the D0 detector and correspond to an integrated luminosity of 3.7(7.3) fb $^{-1}$  for the electron (muon) channel respectively.

The events are selected for the electron or muons and atleast one hadronic decays of  $\tau$  and one good jet. For electron channel, a neural-network to reject  $t\bar{t}$ , and  $D_{MJ}$  to reject MJ. For muon channel, most of the MJ background is removed by the requirement  $D_{MJ} > 0.1$ , where  $D_{MJ}$  is a multivariate discriminant described below. Finally, to improve the signal background ratio, we select a more restrictive b-tagged sample by demanding at least one jet to have  $NN_b > 0.25$ . This b-tag requirement has an efficiency of 65% for a probability of misidentifying a light jet as a b jet of 5%. The number of expected SM background events (the number of observed data) are 2660.8(2629), 476.0(488) for  $e$  or  $\mu\tau_{had}b$  channel. For  $\mu\tau_{had}b$ , a discriminant to reject  $t\bar{t}$  and  $M_{hat}$  variable is defined as the energy of  $\tau_h\mu$  and its momentum along beam axis. We use a multivariate technique with these variables in order to discriminate signal from background which is shown in Fig. 3 for both channels.. Eventually, the data are compatible with the background expectation for the final discriminant and we proceed to set limits on production cross-section. Some of the major systematic uncertainty contribution comes from MJ estimation 10-40%,  $Z + b$ -tagged jets normalizations(5%), jet energy calibration (10%) and b-tagging (4%) in addition to the uncertainty mentioned in above analysis.

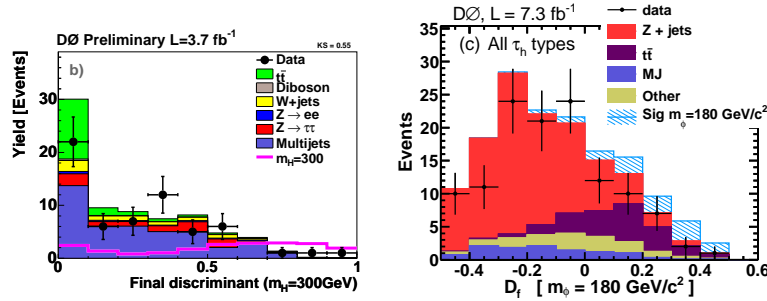


FIG. 3: Final discriminant shape is shown for electron (left) and muon (right) channel.

### IV. RESULTS

Visible mass distribution for the analysis is used as input to a significance calculation using a modified frequentist approach with a Poisson log-likelihood ratio test statistic. In the absence of a significant signal, we derive upper limits for neutral Higgs boson production cross-section and a profiling technique to reduce systematic uncertainties. The confidence level,  $CL_s$  is defined as  $CL_s = CL_{s+b}$  divided by  $CL_b$ , where  $CL_{s+b}$  and  $CL_b$  are the confidence levels in the signal+background and background only hypothesis. The combined limit on the mass of neutral Higgs boson is set from  $m_A = 90-250$  GeV. An example fit in CDF inclusive search is also shown in Fig. 4. We observe no signal evidence in  $m_A = 90-250$  GeV. The sensitivity assuming no signal is shown in and denoted as expected limits. Similarly, limit on the mass of neutral Higgs boson is set from  $m_A = 90-320$  GeV for muon channel (90-320 GeV for electron channel) with the complimentary channels as shown in Fig. 7. These limits are translated into  $\tan\beta$ ,  $m_A$  plane for two MSSM benchmark scenarios the  $m_h^{max}$  and no mixing scenarios with  $\mu > 0$  or  $\mu < 0$  and shown in Fig. 5, 6 for inclusive production. The exclusion plots in same parameter plane is shown in also Higgs production associated with a b quark electron and muon channel

is shown Fig. 8, 9. We exclude a substantial region of the MSSM parameter space, especially at low  $m_A$  and set the most stringent limit to date at the Tevatron, involving  $\tau$  final states.

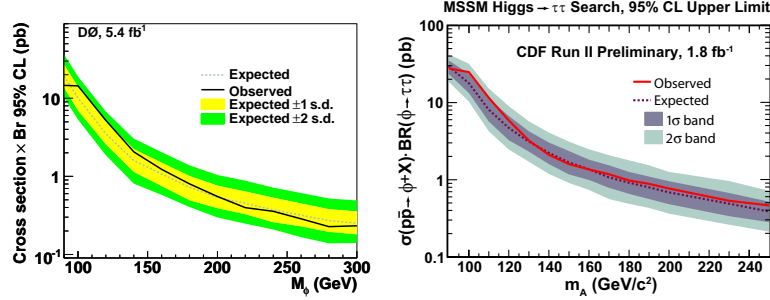


FIG. 4: Observed and expected limits at 95% CL for Higgs production cross-section times branching ratio to  $\tau$  pairs, CDF (right) and D0 (left)

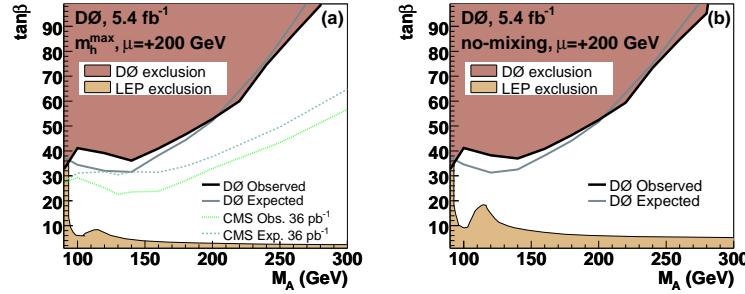


FIG. 5: Excluded region in  $\tan\beta$  vs  $m_A$  plane for the  $m_h^{max}$  with  $\mu > 0$  (left) and no-mixing scenarios with  $\mu < 0$  (right) for D0

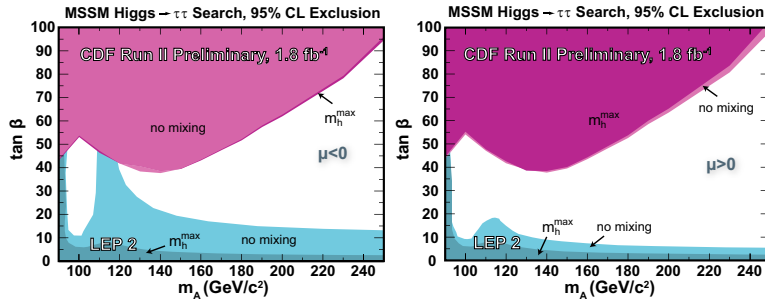


FIG. 6: Excluded region in  $\tan\beta$  vs  $m_A$  plane for the  $m_h^{max}$  and no-mixing scenarios with  $\mu > 0$  and  $\mu < 0$  for CDF

- 
- [1] H. P. Nilles. Phys. Rep. 110 1(1984); H. E. Haber and G. L. Kane Phys. Rep. 117 75(1985)
  - [2] V. M. abazov et al. (D0 collaboration); Nucl. instrum. Methods Phys. Res. A 565, 463 (2006); D. Acosta et al. Phys. rev. D71 032001 (2005)
  - [3] <http://www-d0.fnal.gov/Run2Physics/WWW/results/final/HIGGS/H11D/> arXiv:1106.4555
  - [4] [http://www-cdf.fnal.gov/~aa/mssm\\_htt/index.htm](http://www-cdf.fnal.gov/~aa/mssm_htt/index.htm)
  - [5] <http://www-d0.fnal.gov/Run2Physics/WWW/results/prelim/HIGGS/H104/>, V. M. abazov et al. Phys. Rev. Lett. 107, 121801 (2011)

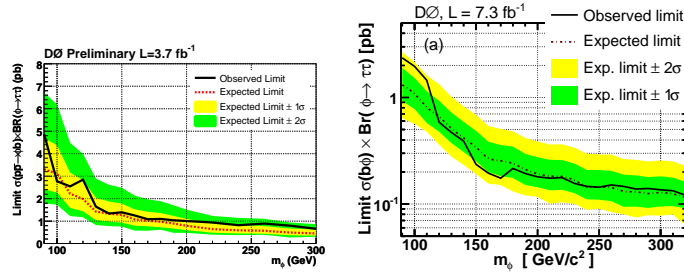


FIG. 7: Observed and expected limits at 95% CL for Higgs production cross-section times branching ratio to  $\tau$  pairs, muon (right) and electron channel at D0 (left)

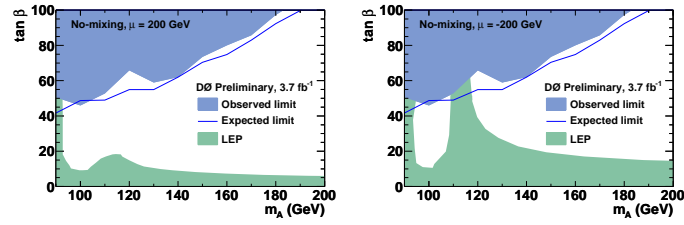


FIG. 8: Excluded region in  $\tan\beta$  vs  $m_A$  plane for the  $m_h^{max}$  and no-mixing scenarios with  $\mu > 0$  and  $\mu < 0$  for D0 in electron channel

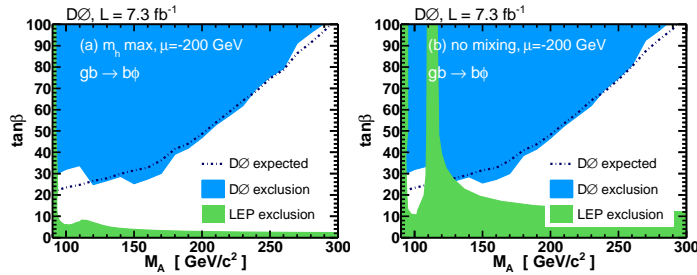


FIG. 9: Excluded region in  $\tan\beta$  vs  $m_A$  plane for the no-mixing scenarios with  $\mu > 0$  (left) and  $\mu < 0$  (right) for D0 in muon channel